Journal of Geophysical Research: Atmospheres

Supporting Information for

Skillful Subseasonal Forecasts of Weekly Tornado and Hail Activity using the Madden-Julian Oscillation

Cory F. Baggett[1], Kyle M. Nardi[1], Samuel J. Childs[1], Samantha N. Zito[2], Elizabeth A. Barnes[1], and Eric D. Maloney[1]

[1] Department of Atmospheric Science, Colorado State University, Fort Collins, CO, USA

[2] School of Marine and Atmospheric Sciences, Stony Brook University, Stony Brook, NY, USA

Contents of this file

Introduction

In Text S1, we demonstrate the robustness of our results to the heterogeneities found in the storm reports. In Text S2, we provide the locations of the data repositories used in this study. In the supporting figures, we display Figure 2 with its statistical significance plotted and the plotting function's smoothing turned off (Figure S1); skill scores of forecasts for severe weather variables using a leave-three-years-out cross validation rather than a leave-one-year-out cross validation (Figure S2); composites of severe weather variables based on the RMM index rather than the OMI (Figure S3); skill scores of forecasts for severe weather variables based on the RMM index rather than the OMI (Figure S4); composites of tornado and hail reports rather than events (Figure S5); skill scores of forecasts for tornado and hail reports rather than events (Figure S6); and composites of tornado and hail events for the sub-periods of 1979-1996 and 1997-2015 (Figure S7). In Table S1, we provide sample sizes for the number of days in each MJO phase.

Text S1. Sensitivity of the results to heterogeneities in the storm reports

There are well-documented, non-meteorological heterogeneities that influence the upward trends seen in the numbers of tornado and severe hail reports in recent years, primarily related to population growth, denser road networks, an increasing number of storm chasers, and changes in reporting criteria (Agee & Childs, 2014; Allen & Tippett, 2015). Because we are primarily concerned with the subseasonal variability of convective severe weather rather than its interannual variability, these heterogeneities in the storm reports are not expected to be excessively deleterious. With respect to the tornado reports, the non-meteorological influence is diminished greatly by restricting our analysis to only tornado reports with intensities of EF1 or

41 greater because they show no discernible annual trend, as opposed to the inclusion of EF0
42 tornadoes which display a discontinuous upward jump in the 1990s associated with the advent of
43 Doppler radar (Agee & Childs, 2014; Tippett et al., 2015). With respect to both tornado and hail
44 reports, Allen and Tippett (2015) suggests three tests to gauge the robustness of an analysis to
45 heterogeneities, all of which we perform in this study. First, reports can be analyzed in the
46 context of events rather than total number of reports. We test the sensitivity of our analysis to
47 using reports instead of events and find little qualitative difference (compare Figures 2 and 5 to
48 Figures S5 and S6, respectively). Second, the analysis can be performed on a subsampling of
49 time periods. In Figures S7, we compare the two sub-periods of 1979–1996 and 1997–2015.
50 While there is little qualitative difference between the two sub-periods in the Plains, there are
51 differences evident in the Southeast. These differences likely explain the higher predictive skill
52 of the empirical prediction model in the Plains versus the Southeast (compare Figures 5d,e to
53 Figures 5i,j). Third, and perhaps most importantly, environmental parameters important to severe
54 weather activity can serve as proxies to the actual storm reports (Allen et al., 2015). We analyze
55 CAPE, SRH, and CSRH2 throughout this study and find their subseasonal behavior to be
56 consistent with that of the tornado and hail events (Figures 2 and 5).
57
58 **Text S2. Data availability**
59 ERA-Interim data (Dee et al., 2011) were obtained on 8 September 2016 and are
60 available from the ECMWF public data set portal (http://apps.ecmwf.int/datasets/data/interim-
61 full-daily/levtype=sfc/).

Tornado and hail reports data (Schaefer & Edwards, 1999) were obtained on 7 August 2017 and are available from the SPC's Severe Weather Database, archived at the National Centers for Environmental Information (https://www.ncdc.noaa.gov/stormevents/).

The OMI (Kiladis et al., 2014) was obtained on 6 January 2017 and is available from NOAA Earth System Research Laboratory Physical Sciences Division (https://www.esrl.noaa.gov/psd/mjo/mjoindex/).

The RMM index (Wheeler & Hendon, 2004) was obtained on 11 October 2016 and is available from the Australian Government Bureau of Meteorology (http://www.bom.gov.au/climate/mjo/).

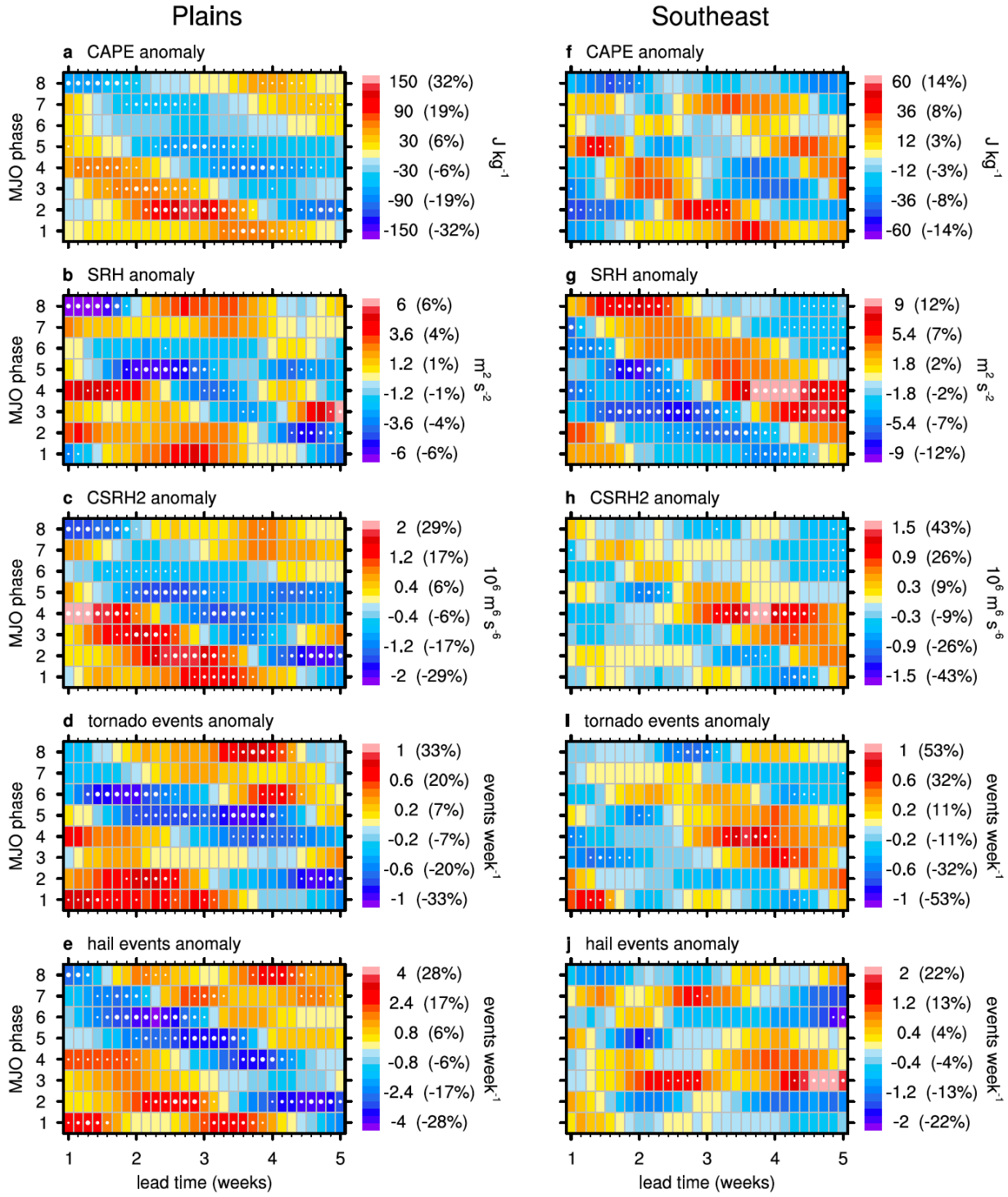
Plains
Southeast
a CAPE anomaly
150 (32%)
90 (19%)
30 (6%)
-30 (-6%)
-90 (-19%)
-150 (-32%)
J kg-1
f CAPE anomaly
60 (14%)
36 (8%)
12 (3%)
-12 (-3%)
-36 (-8%)
-60 (-14%)
J kg-1
b SRH anomaly
6 (6%)
3.6 (4%)
1.2 (1%)
-1.2 (-1%)
-3.6 (-4%)
-6 (-6%)
m2 s-2
g SRH anomaly
9 (12%)
5.4 (7%)
1.8 (2%)
-1.8 (-2%)
-5.4 (-7%)
-9 (-12%)
m2 s-2
c CSRH2 anomaly
2 (29%)
1.2 (17%)
0.4 (6%)
-0.4 (-6%)
-1.2 (-17%)
-2 (-29%)
10^6 m^6 s^-6
h CSRH2 anomaly
1.5 (43%)
0.9 (26%)
0.3 (9%)
-0.3 (-9%)
-0.9 (-26%)
-1.5 (-43%)
10^6 m^6 s^-6
d tornado events anomaly
1 (33%)
0.6 (20%)
0.2 (7%)
-0.2 (-7%)
-0.6 (-20%)
-1 (-33%)
events week-1
l tornado events anomaly
1 (53%)
0.6 (32%)
0.2 (11%)
-0.2 (-11%)
-0.6 (-32%)
-1 (-53%)
events week-1
e hail events anomaly
4 (28%)
2.4 (17%)
0.8 (6%)
-0.8 (-6%)
-2.4 (-17%)
-4 (-28%)
events week-1
j hail events anomaly
2 (22%)
1.2 (13%)
0.4 (4%)
-0.4 (-4%)
-1.2 (-13%)
-2 (-22%)
events week-1
MJO phase
1 2 3 4 5 6 7 8
1 2 3 4 5
lead time (weeks)

71

Figure S1. As in Figure 2 but with its statistical significance plotted and the plotting function's smoothing turned off. Statistical significance is conveyed by small, medium, and large white dots for composites of MJO phase and lead time that are more skillful than 80%, 90%, and 95%, respectively, of 1000 random composites generated by a bootstrapping technique that accounts for autocorrelation (see Section 2.6).

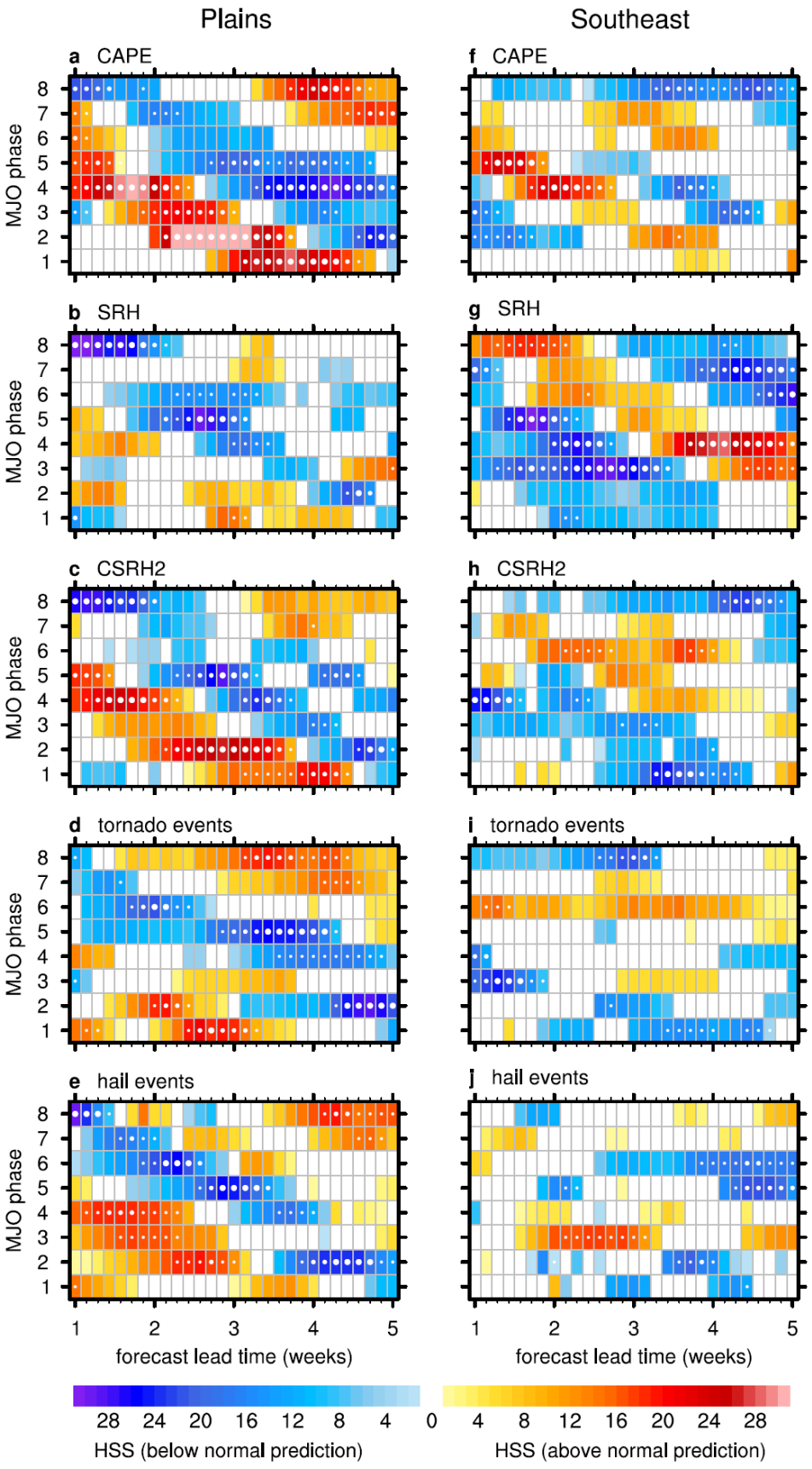
Plains
Southeast
a CAPE
f CAPE
b SRH
g SRH
c CSRH2
h CSRH2
d tornado events
i tornado events
e hail events
j hail events
MJO phase
1 2 3 4 5 6 7 8
forecast lead time (weeks)
28 24 20 16 12 8 4 0
HSS (below normal prediction)
0 4 8 12 16 20 24 28
HSS (above normal prediction)

77

Figure S2. As in Figure 5, except the Heidke skill scores of the empirical prediction model for leave-three-years-out cross validation rather than leave-one-year-out cross validation are shown for (**a**,**f**) CAPE, (**b**,**g**) SRH, (**c**,**h**) CSRH2, (**d**,**i**) tornado events, and (**e**,**j**) hail events for the (**a-e**) Plains and (**f-j**) Southeast. Forecasts are issued for 12 consecutive, non-overlapping three-year periods. These forecasts are generated from each period's respective training period of 34 left-out years. For example, the years 1982–2015 constitute the training period used to generate a forecast for 1979–1981; and the years 1979–2011 and 2015 are used to generate a forecast for 2012–2014.

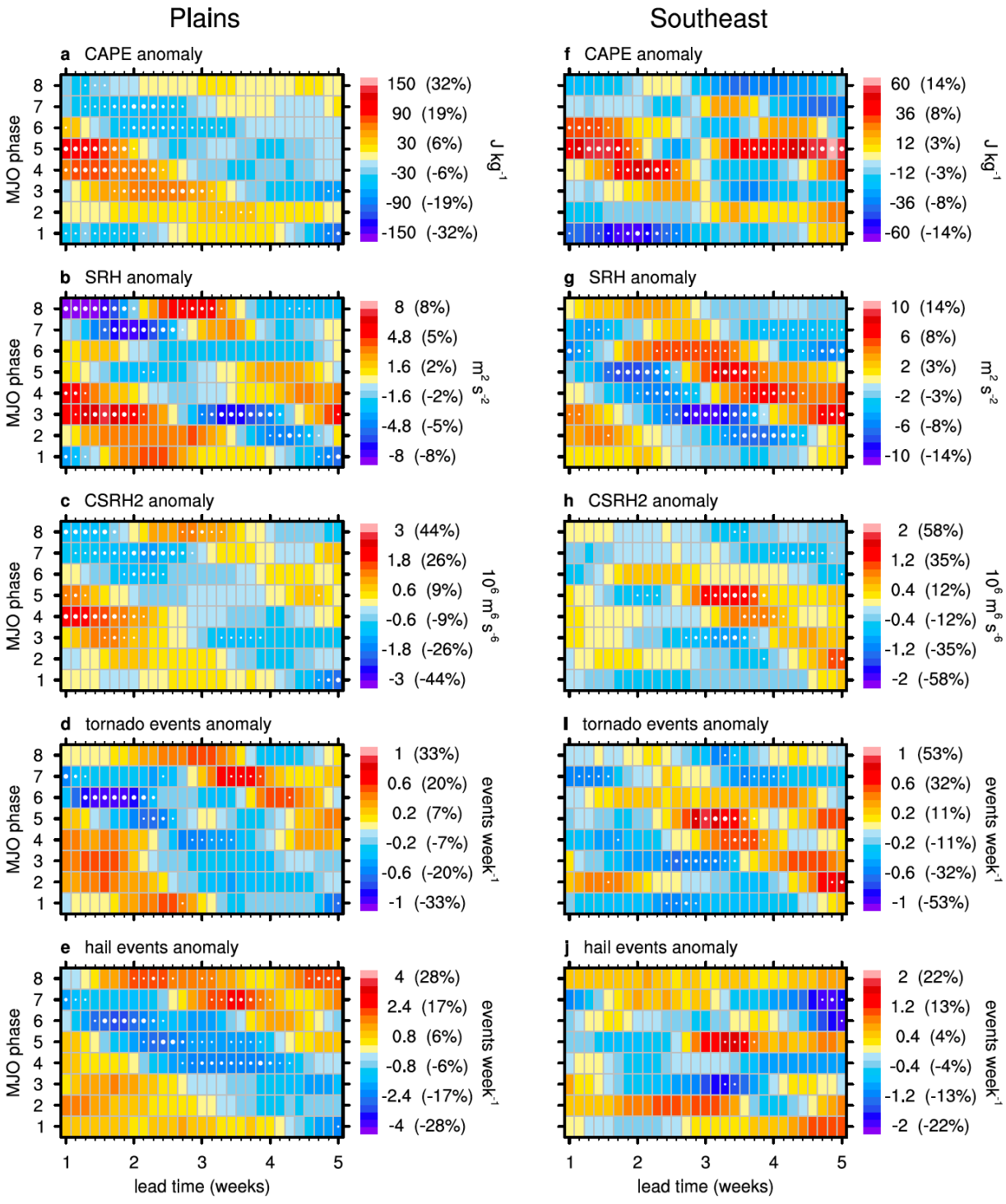
Plains
Southeast
a CAPE anomaly
b SRH anomaly
c CSRH2 anomaly
d tornado events anomaly
e hail events anomaly
f CAPE anomaly
g SRH anomaly
h CSRH2 anomaly
i tornado events anomaly
j hail events anomaly
MJO phase
lead time (weeks)
J kg-1
m2 s-2
10^6 m^6 s^-6
events week-1
150 (32%)
90 (19%)
30 (6%)
-30 (-6%)
-90 (-19%)
-150 (-32%)
8 (8%)
4.8 (5%)
1.6 (2%)
-1.6 (-2%)
-4.8 (-5%)
-8 (-8%)
3 (44%)
1.8 (26%)
0.6 (9%)
-0.6 (-9%)
-1.8 (-26%)
-3 (-44%)
1 (33%)
0.6 (20%)
0.2 (7%)
-0.2 (-7%)
-0.6 (-20%)
-1 (-33%)
4 (28%)
2.4 (17%)
0.8 (6%)
-0.8 (-6%)
-2.4 (-17%)
-4 (-28%)
60 (14%)
36 (8%)
12 (3%)
-12 (-3%)
-36 (-8%)
-60 (-14%)
10 (14%)
6 (8%)
2 (3%)
-2 (-3%)
-6 (-8%)
-10 (-14%)
2 (58%)
1.2 (35%)
0.4 (12%)
-0.4 (-12%)
-1.2 (-35%)
-2 (-58%)
1 (53%)
0.6 (32%)
0.2 (11%)
-0.2 (-11%)
-0.6 (-32%)
-1 (-53%)
2 (22%)
1.2 (13%)
0.4 (4%)
-0.4 (-4%)
-1.2 (-13%)
-2 (-22%)

86

87 **Figure S3.** As in Figure S1, except composites based on the RMM index rather than the OMI are
88 shown for anomalous (**a**,**f**) CAPE, (**b**,**g**) SRH, (**c**,**h**) CSRH2, (**d**,**i**) tornado events, and (**e**,**j**) hail
89 events for the (**a**-**e**) Plains and (**f**-**j**) Southeast.

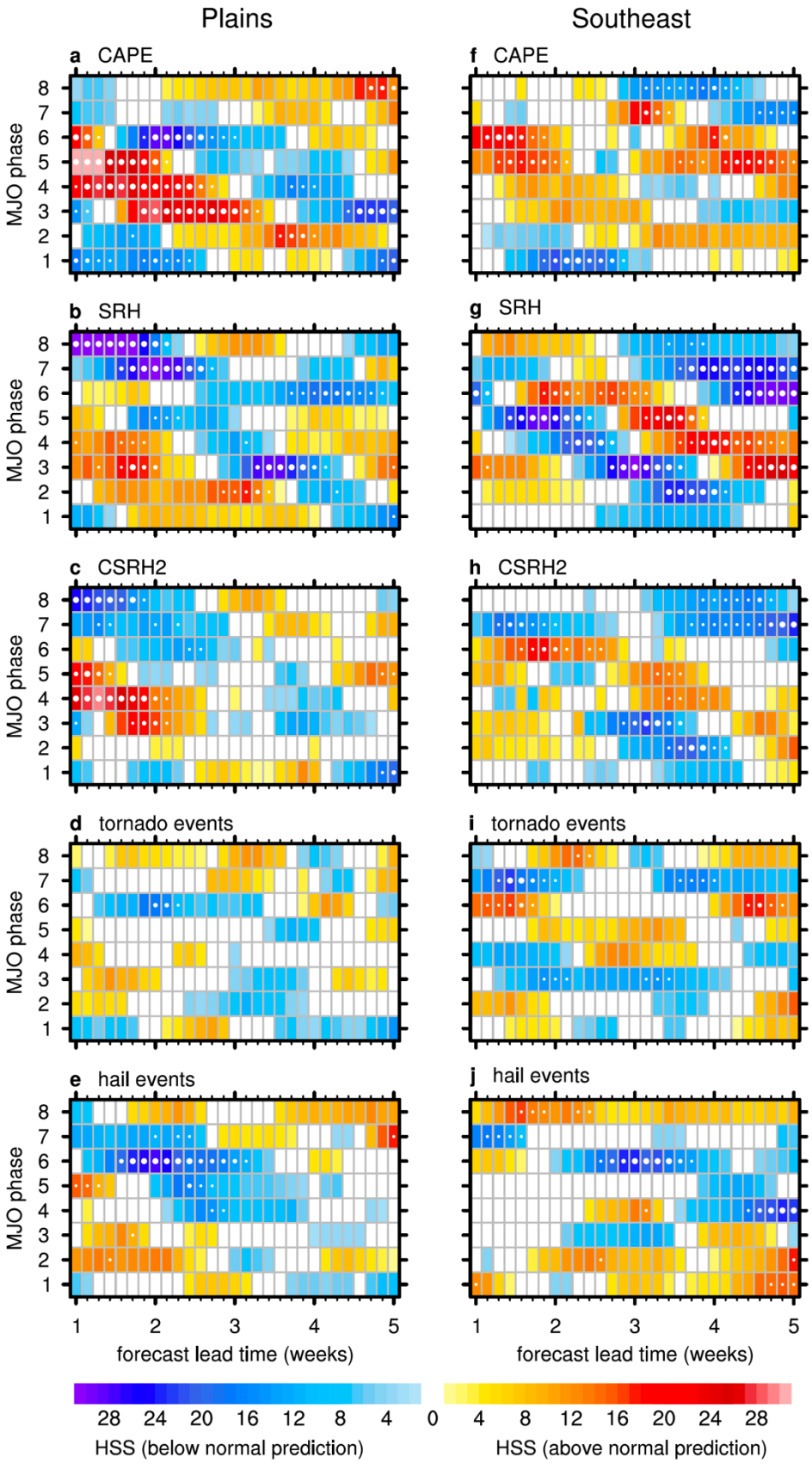
Plains
Southeast
a CAPE
f CAPE
b SRH
g SRH
c CSRH2
h CSRH2
d tornado events
i tornado events
e hail events
j hail events
MJO phase
1 2 3 4 5 6 7 8
forecast lead time (weeks)
28 24 20 16 12 8 4 0 4 8 12 16 20 24 28
HSS (below normal prediction)
HSS (above normal prediction)

90

Figure S4. As in Figure 5, except Heidke skill scores of the empirical prediction model based on the RMM index rather than the OMI are shown for (**a**,**f**) CAPE, (**b**,**g**) SRH, (**c**,**h**) CSRH2, (**d**,**i**) tornado events, and (**e**,**j**) hail events for the (**a-e**) Plains and (**f-j**) Southeast.

94

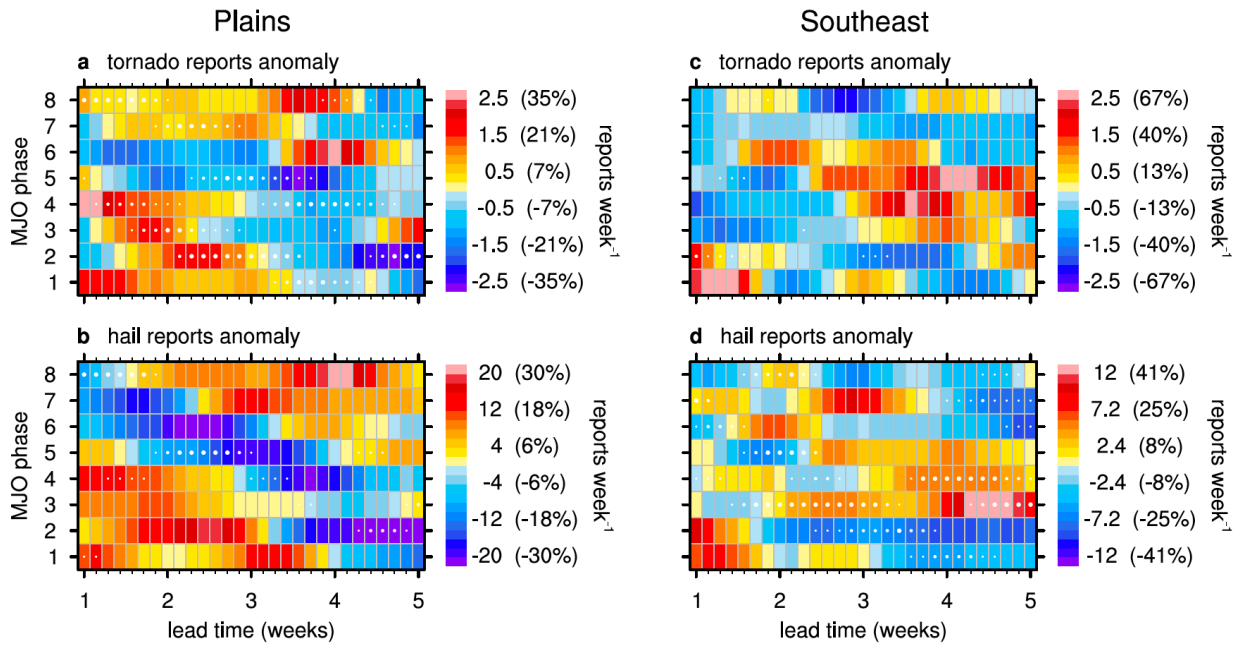
Plains
Southeast
a tornado reports anomaly
b hail reports anomaly
c tornado reports anomaly
d hail reports anomaly
MJO phase
lead time (weeks)
reports week^{-1}
2.5 (35%)
1.5 (21%)
0.5 (7%)
-0.5 (-7%)
-1.5 (-21%)
-2.5 (-35%)
20 (30%)
12 (18%)
4 (6%)
-4 (-6%)
-12 (-18%)
-20 (-30%)
2.5 (67%)
1.5 (40%)
0.5 (13%)
-0.5 (-13%)
-1.5 (-40%)
-2.5 (-67%)
12 (41%)
7.2 (25%)
2.4 (8%)
-2.4 (-8%)
-7.2 (-25%)
-12 (-41%)

95

Figure S5. As in Figure S1, except composites are shown of anomalous (**a**,**c**) tornado reports and (**b**,**d**) hail reports rather than tornado events and hail events for the (**a**,**b**) Plains and (**c**,**d**) Southeast.

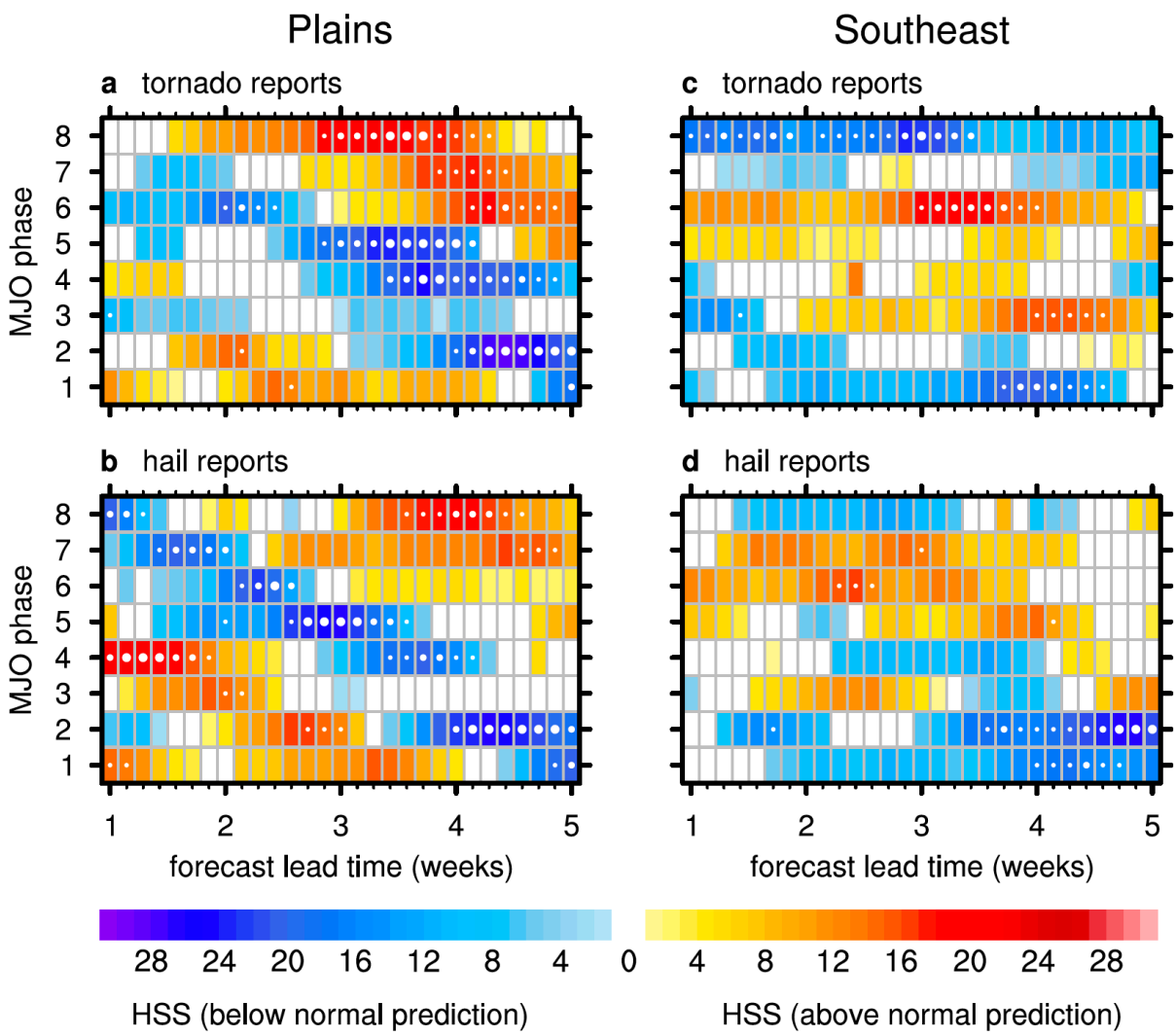
Plains
Southeast
a tornado reports
c tornado reports
b hail reports
d hail reports
MJO phase
forecast lead time (weeks)
28 24 20 16 12 8 4 0 4 8 12 16 20 24 28
HSS (below normal prediction)
HSS (above normal prediction)

99

Figure S6. As in Figure 5, except Heidke skill scores of the empirical prediction model are shown for (**a**,**c**) tornado reports and (**b**,**d**) hail reports rather than tornado events and hail events for the (**a**,**b**) Plains and (**c**,**d**) Southeast.

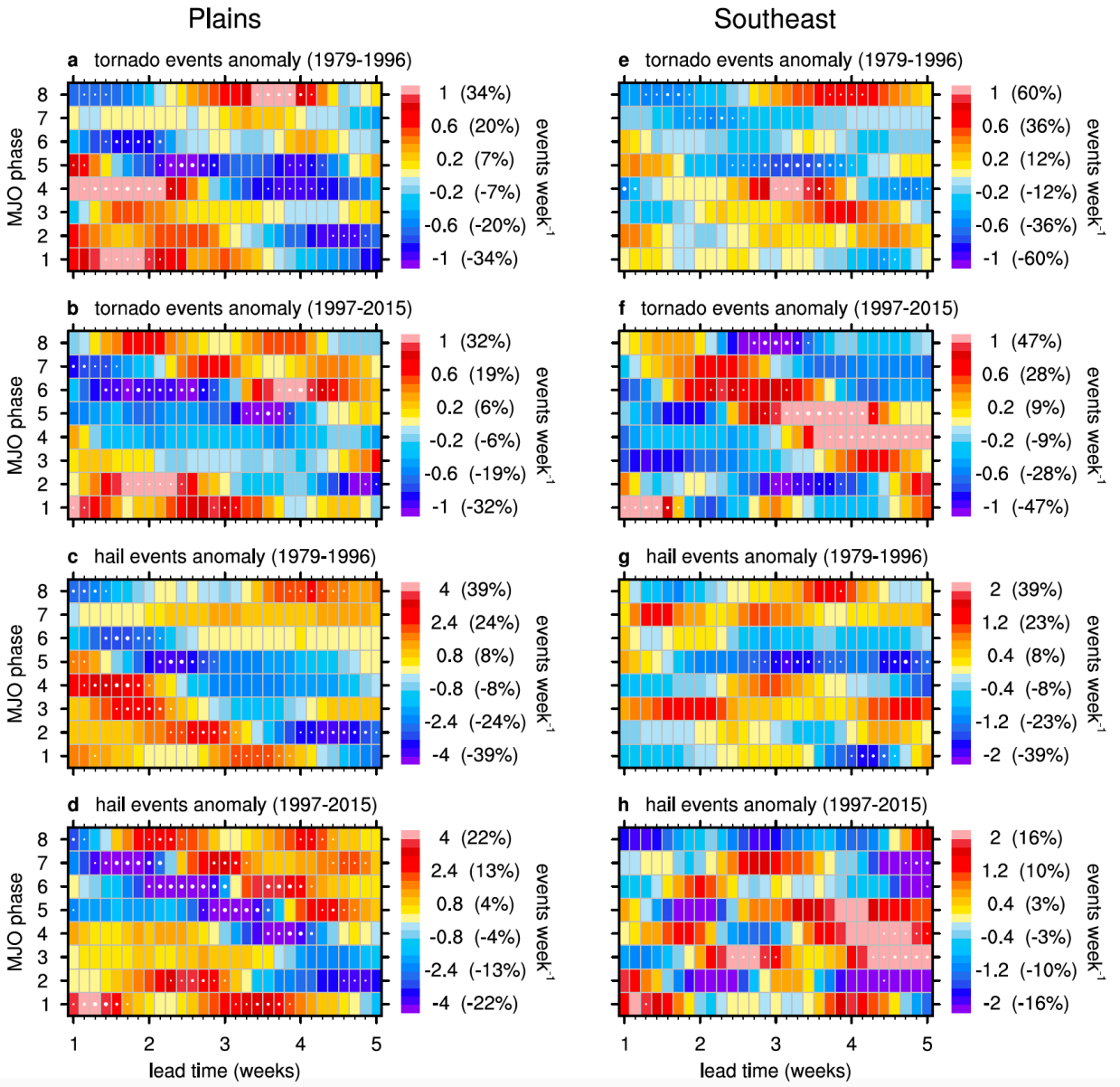
Plains
Southeast
a tornado events anomaly (1979-1996)
b tornado events anomaly (1997-2015)
c hail events anomaly (1979-1996)
d hail events anomaly (1997-2015)
e tornado events anomaly (1979-1996)
f tornado events anomaly (1997-2015)
g hail events anomaly (1979-1996)
h hail events anomaly (1997-2015)
MJO phase
lead time (weeks)
events week^{-1}
1 (34%)
0.6 (20%)
0.2 (7%)
-0.2 (-7%)
-0.6 (-20%)
-1 (-34%)
1 (32%)
0.6 (19%)
0.2 (6%)
-0.2 (-6%)
-0.6 (-19%)
-1 (-32%)
4 (39%)
2.4 (24%)
0.8 (8%)
-0.8 (-8%)
-2.4 (-24%)
-4 (-39%)
4 (22%)
2.4 (13%)
0.8 (4%)
-0.8 (-4%)
-2.4 (-13%)
-4 (-22%)
1 (60%)
0.6 (36%)
0.2 (12%)
-0.2 (-12%)
-0.6 (-36%)
-1 (-60%)
1 (47%)
0.6 (28%)
0.2 (9%)
-0.2 (-9%)
-0.6 (-28%)
-1 (-47%)
2 (39%)
1.2 (23%)
0.4 (8%)
-0.4 (-8%)
-1.2 (-23%)
-2 (-39%)
2 (16%)
1.2 (10%)
0.4 (3%)
-0.4 (-3%)
-1.2 (-10%)
-2 (-16%)

103

Figure S7. As in Figure S1, except composites for the sub-periods of 1979–1996 and 1997–2015 rather than 1979–2015 are shown for anomalous (**a**,**b**,**e**,**f**) tornado events and (**c**,**d**,**g**,**h**) hail events for the (**a**-**d**) Plains and (**e**-**h**) Southeast during the sub-periods of (**a**,**c**,**e**,**g**) 1979–1996 and (**b**,**d**,**f**,**h**) 1997–2015.

a OMI MJO Phase	Sample Size	
	n	n_{eq}
1	298	65
2	315	62
3	389	69
4	318	70
5	291	68
6	376	82
7	402	76
8	332	74

b RMM MJO Phase	Sample Size	
	n	n_{eq}
1	407	101
2	351	97
3	337	90
4	358	100
5	324	91
6	347	83
7	353	90
8	397	96

Table S1. The number of days *n* (sample size) that the MJO resides in each phase with an amplitude ≥ 1 during March-June are shown for (**a**) the OMI and (**b**) the RMM index. The MJO typically resides in a particular phase with an amplitude ≥ 1 for "blocks" of consecutive days in a row. The number of these unique blocks n_{eq} (equivalent sample size) are shown for (**a**) the OMI and (**b**) the RMM index. When calculating statistical significance (see Section 2.6), n_{eq} is used to account for the inherent autocorrelation that the MJO exhibits.